Separation Science and Technology
Publication details, including instructions for authors and subscription information:
http://www.informaworld.com/smpp/title~content=t713708471

The Influence of Retention on the Plate Height in Ion-Exchange Chromatography

Ernst Hansen[ab]; Jørgen M. Mollerup[a]
[a] Department of Chemical Engineering, Engineering Research Centre IVC-SEP, Technical University of Denmark, Lyngby, Denmark [b] Novozymes, Smørmosevej, Bagsværd, Denmark

Online publication date: 08 July 2010

To cite this Article Hansen, Ernst and Mollerup, Jørgen M.(2005) 'The Influence of Retention on the Plate Height in Ion-Exchange Chromatography', Separation Science and Technology, 39: 9, 2011 — 2030
To link to this Article: DOI: 10.1081/SS-120037393
URL: http://dx.doi.org/10.1081/SS-120037393

SEPARATION SCIENCE AND TECHNOLOGY
Vol. 39, No. 9, pp. 2011–2030, 2004

The Influence of Retention on the Plate Height in Ion-Exchange Chromatography

Ernst Hansen[#] and Jørgen M. Mollerup[*]

Department of Chemical Engineering, Engineering Research Centre IVC-SEP, Technical University of Denmark, Lyngby, Denmark

ABSTRACT

The plate heights for the amino acid tyrosine (anion exchange) and the polypeptide aprotinin (cation exchange) were determined on a porous media (Resource 15) and a gel filled media (HyperD 20) at salt concentrations ranging from weak to strong retention. At a constant velocity, measurements showed that the plate height increase with increasing retention, went through a maximum, and finally, decreased as the retention increased, i.e., when the salt concentration was lowered further. The band broadening of a chromatographic peak in the column was caused by the axial dispersion and mass transfer. In this article, the rate of mass transfer in the particles is described by three different rate mechanisms,

[#]Present address: Novozymes, Smørmosevej, 2880 Bagsværd, Denmark; E-mail: eha@novozymes.com.
[*]Correspondence: Jørgen M. Mollerup, Department of Chemical Engineering, Engineering Research Centre IVC-SEP, Technical University of Denmark, DTU Building 229, 2800Lyngby, Denmark; Fax: +45-4588-2258; E-mail: jm@kt.dtu.dk.

2011

DOI: 10.1081/SS-120037393 0149-6395 (Print); 1520-5754 (Online)

pore diffusion, solid diffusion, and parallel diffusion. The van Deemter equation was used to model the data to determine the mass-transfer properties. The development of the plate height with increasing retention revealed a characteristic behavior for each rate mechanism. In the pore diffusion model, the plate height increased toward a constant value at strong retention, while the plate height in the solid diffusion model decreased, approaching a constant value at strong retention. In the parallel diffusion model, both pore and solid diffusion took place. Therefore, the parallel diffusion model coincides with the pore diffusion model at weak retention and with the solid diffusion model at strong retention, while a maximum is reached at intermediate retention, resulting in a bell-shaped curve. This behavior corresponds to the observed variation of the plate height at constant velocity. Neither the pore nor the solid diffusion model can describe the experimental data while a satisfactory fit was obtained using the parallel diffusion model.

Key Words: Plate height; Mass-transfer behavior; van Deemter equation; Ion-exchange chromatography.

INTRODUCTION

At linear adsorbing conditions, the plate height (HETP) was determined from the variance of the response to a pulse injection. The plate height depends on the velocity, the rate of mass transfer, the retention behavior, as well as the particle diameter and the porosities. The experimental data for the plate height were correlated by the van Deemter equation. The plate height had an explicit and an implicit dependence on the retention because the rate of mass transfer depended on the equilibrium conditions. The scope of this study was to determine how the plate height varies with the retention and use of the van Deemter equation to investigate different models for mass transfer. The plate height for tyrosine and aprotinin were measured over a wide range of salt concentrations, ranging from weak to strong retention, on two different resins, a porous media (Resource 15Q&S) and a gel-filled media (Q&S HyperD 20). When the isotherm was linear, the overall mass-transfer resistance was the sum of the film resistance and the intraparticle resistance. The model for intraparticle mass transfer can include either pore diffusion, solid diffusion, or both, usually referred to as parallel diffusion. Often, the overall mass-transfer resistance is determined by measuring the plate height as a function of the velocity under nonretained conditions.[1–3] However, from experiments performed at a constant retention, the nature of the rate mechanism in the particles cannot be determined since the plate height at a constant retention can be matched by any of the three models. Therefore, to

distinguish between the various mass-transfer mechanisms, the plate height must be determined at conditions having a significant variation in the retention.

THEORY

The van Deemter equation[4] Eqs. (34)–(38) is used to model plate height data. The rate of mass transfer is described by the linear driving force approximation. Because of the small diffusion coefficients of the solutes, tyrosine and aprotinin, the contribution from ordinary diffusion to the band broadening can be neglected. When the column to particle diameter ratio is above 200, experiments show[5] that the eddy diffusion coefficient is proportional to the velocity. Using these assumptions, the reduced plate height $h = H/d_p$ given by the van Deemter equation is[4]

$$h = 2\lambda + 2\left(\frac{k'}{1+k'}\right)^2 \frac{\varepsilon v}{6(1-\varepsilon)K_m} = 2\lambda + 2\left(\frac{1+A}{p+1+A}\right)^2 \frac{\varepsilon v}{6(1-\varepsilon)K_m} \tag{1}$$

λ is a constant, usually between 1 and 3, related to the axial dispersion coefficient, $D_{ax} = \lambda v d_p$ and $p = \varepsilon/(1-\varepsilon)K_d\varepsilon_p$ is in the order of 1 to 2. K_m is the overall mass-transfer coefficient corresponding to an overall linear driving force in the liquid phase concentration $C - C_{pore}$ and $A = q/C_{pore}$ is the equilibrium ratio between the adsorbed and pore phase concentrations in the particle. The adsorbed and pore phase concentrations are defined with respect to the accessible pore volume, with the retention factor $k' = (1-\varepsilon)K_d\varepsilon_p (1+A)/\varepsilon$. The development of the plate height with increasing retention depends on the retention factor as well as the variation of the overall mass-transfer coefficient as discussed as follows. A discussion of intraparticle mass transfer is available in *Perry's Handbook*.[6]

A word of caution regarding flow in a packed bed and the eddy diffusion coefficient. Chu and Ng[7] showed that for a tube to particle diameter ratio larger than 25, the permeability is the same as that of a large diameter tube. When the ratio is between 8 and 25, the permeability can be larger or less than that of a large diameter tube. The way the tube is packed determines whether the higher porosity or surface area dominates in the wall region, and thus higher or lower permeability. When the ratio is below 8, the confining wall causes a marked increase in the overall bed porosity and the permeability is always larger than that of a large diameter column. Chung and Wen[8] report similar results. The wall region extends about 0.5-particle diameters from the wall for particles of normal imperfection of size and shape.[9] Like ordinary

diffusion eddy diffusion is a second-order effect and a uniform permeability is a necessary but by far a sufficient criterion to ensure that the eddy diffusion becomes proportional to the velocity at low to moderate velocities, finding a constant Péclet number for the particle. If the wall region is less than 1% of the total flow area, the column to particle diameter must be larger than 200, or as Yamamoto phrases it: "When the column–particle diameter ratio is above 200, the column efficiency is not markedly varied."[5] Knox[10] presented his view on eddy diffusion and the van Deemter equation, but some of his conclusions are based on experiments in columns having a column–particle diameter ratio less than 200. Following Chung and Wen,[8] we assumed that the particle Péclet number is velocity independent for Reynolds numbers less than 1 and thus $D_{ax} = \lambda v d_p$ when the column to particle diameter ratio is above 200.

Pore Diffusion

When the isotherm is linear, the overall mass-transfer coefficient K_m is calculable from the sum of the resistances due to mass transfer in the film and in the particle. The resistance is the reciprocal of the mass-transfer coefficient. When the intraparticle mass transfer is controlled by pore diffusion, the overall mass-transfer coefficient is

$$\frac{1}{K_m} = \frac{1}{k_f} + \frac{1}{K_d \varepsilon_p k_p} \tag{2}$$

k_f is a velocity-dependent film mass-transfer coefficient for the external mass transfer and k_p is the pore-phase mass-transfer coefficient. The product $K_d\varepsilon_p$ is the effective particle porosity for a given solute. Since the overall mass-transfer coefficient for pore diffusion is a constant at fixed velocity, the plate height for pore diffusion will increase when equilibrium ration A increases and approach a constant value when the term in the brackets of Eq. (1) approaches unity, as shown in Fig. 1.

Solid Diffusion

In solid diffusion, the driving force for mass transfer is the apparent difference in the adsorbed phase concentration q. When the isotherm is linear, the overall mass-transfer coefficient is calculable as

$$\frac{1}{K_m} = \frac{1}{k_f} + \frac{1}{K_d \varepsilon_p A k_q} \tag{3}$$

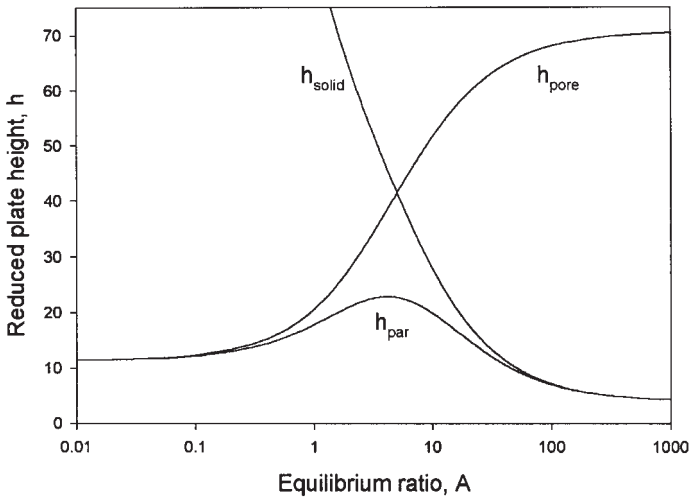

Figure 1. The plate height behavior for pore, solid, and parallel diffusion calculated from Eqs. (1) and (2)–(4) with $\varepsilon = 0.5$, $\varepsilon_p = 0.5$, $\lambda = 2$, $k_p = 2 \times 10^{-3}$ cm/sec, and $k_q = 0.4 \times 10^{-3}$ cm/sec at $v_0 = 0.1$ cm/sec. The film resistance is not included.

k_q is the solid-phase mass-transfer coefficient and $A = q/c$. Inserting this expression in the van Deemter equation shows that the plate height for solid diffusion decreases when A increases and approaches a constant value for large values of A. A deficiency of the solid diffusion model is that the plate height approaches infinity at nonretained conditions where A approaches 0, as shown in Fig. 1.

Parallel Diffusion

In the parallel diffusion model, the intraparticle mass transfer is caused by pore and solid diffusion simultaneously, i.e., the two mechanism work in parallel.

$$\frac{1}{K_m} = \frac{1}{k_f} + \frac{1}{K_d \varepsilon_p (k_p + A k_q)} \tag{4}$$

Due to the parallel nature of the transport mode, the rate of mass transfer in the particles will be controlled by the faster mechanism. At low retention, where $k_p \gg A k_q$, the mass transfer is caused by pore diffusion while solid diffusion predominates as the equilibrium ratio A becomes large. Since

the plate height increases with A for low to moderate retention and decreases with A for strong retention, a maximum in the plate height will be reached at an intermediate equilibrium ratio. Finally, it is noted that the pore and solid diffusion models, Eqs. (2) and (3), are limiting cases of the general parallel diffusion model Eq. (4). Knox and co-workers[10,11] investigated the van Deemter equation with a parallel diffusion model.

Figure 1 shows the variation of the reduced plate height with the equilibrium ratio for the three models. For simplicity, the contribution from the external film resistance is not included. At low retention, pore diffusion predominates and the plate height for parallel diffusion $h_{par} \approx h_{pore}$ increases with increasing A, while at strong retention, solid diffusion predominates and $h_{par} \approx h_{solid}$ decreases with increasing A. At intermediate retention, a transition from the pore to the solid diffusion domain takes place and the plate height reaches a maximum, therefore, the resulting variation of h_{par} with A becomes less than the variation for pore or solid diffusion.

Experimental data for the plate height obtained at a constant retention can be matched by any of the three models. Thus from a plot of the plate height vs. the velocity (the so called van Deemter plot), we cannot, in general, distinguish between the various modes of the mass transfer. However, with a significant variation in the equilibrium ratio, a plot of h vs. A at a constant velocity will show a distinguished shape for each of the three models, as shown in Fig. 1. Thus, by determining the plate height as function of the equilibrium ratio, we can investigate the significance of the three models for intraparticle mass transfer.

Equilibrium Ratio

The equilibrium ratio depends on the concentration of the counter ion and is described by the mass action law:[12]

$$A = \frac{q}{c} = K\left(\frac{\Lambda}{c_s}\right)^{z_{solute}/z_{salt}} = B_{c_s^{-ny}} \tag{5}$$

K is the thermodynamic equilibrium constant, Λ is the concentration of equivalents in the adsorbent, c_s is the concentration of the counter ion, and z_{solute} is the effective or binding charge of the solute. For large molecules, such as proteins, where several configurations of attachment are possible, the effective binding charge may depend on the nature of the adsorbent and moderate differences in the charge ratio ν should be expected.

EXPERIMENTAL

Chemicals

Aprotinin, provided by Novo Nordisk (Denmark), is a single-chain polypeptide containing 58 amino acids with a molecular weight of 6512D and an isoelectric point of 10.5. The purity is >99%. Tyrosine (T-3754) and NaAc (S5889) are from Sigma, $NaNO_3$ (1.06537) and NaCl (1.06404) are from Merck, 5 N HCl (Lab00440) and 5 N NaOH (Lab00334) are from Bie & Berntsen (Denmark). Standard solutions for calibration of the pH meter are from Radiometer (pH = 4.01, 7.00, and 10.01).

Equipment

The BioCAD chromatographic workstation is from Perseptive Biosystems, the pH meter (pHM 92) is the Radiometer, 0.45 μm HV filters are from Millipore. Columns: Resource 15S (no. 510566), $30 \times 6.4\,mm^2$ (1 mL), Resource 15S (no. 300734) and 15Q (no. 301572), $30 \times 16\,mm^2$ (6 mL) are from Amersham Biotech. Q HyperD 20 (lot 5155) and S HyperD 20 (lot 4206), $100 \times 4.6\,mm^2$ (1.7 mL) are from BioSepra.

Procedures

The experimental conditions are summarized in Table 1. The aprotinin solutions were prepared by dissolving the acetate buffer and NaCl and adding 5 N HCl to reach pH 5. The tyrosine solutions were prepared by dissolving NaCl and adding 5 N NaOH to reach pH 11. The high pH used in the tyrosine experiments was selected to have a total charge close to −2. Calculation of the Bjerrum[13] diagram for tyrosin shows that it is almost fully dissociated at pH 11. The pH meter was calibrated using standard solutions at pH 4.01 and 7.00 or 7.00 and 10.01. All solutions were filtered through 0.45 μm filters. The pulse response curves were measured at 254 and 280 nm. Solutions for injection were prepared by dissolving the solute in the buffer used as mobile phase. The solute concentrations were 1 g/L for aprotinin and 0.3 g/L for tyrosine. The injection volume was approximately 100 μL. A series of experiments with different injection volumes was performed at low to moderate salt concentrations to verify that the isotherm could be considered linear at these conditions.

Table 1. Parameters and experimental conditions.

	Tyrosine		Aprotinin	
Buffer	None		50 nM NaAc	
pH	11 (NaOH)		5 (HCl)	
c_{feed} (g/L)	0.3		1	
$D \times 10^6$ (cm^2/sec)	10		1.3	
Resin	Resource 15Q	Q HyperD 20	Resource 15S	S HyperD 20
V_{col} (mL)	6	1.7	1 and 6	1.7
d_p (μL)	15	20	15	20
ε	0.48	0.37	0.48	0.37
ε_p	0.51	0.54	0.51	0.54
v_0 (cm/sec)	0.05–0.2	0.1–0.5	0.008–0.2	0.1–0.3
c_{salt} (M)	0.02–1	0.02–0.3	0.15–2.05	0.25–1.05
K_d	1	1	1	0.74
B (M^v)	0.16	0.13	0.01	0.13
v	1.86	1.87	5.52	4.34
λ	1.9	1.2	1.9	1.2
$\alpha \times 10^3$ (cm/sec)$^{1-\beta}$	55	13	9.4	2.2
β	1/3	1/3	1/3	1/3
$k_p \times 10^3$ (cm/sec)	11	11	3.2	0.36
$k_q \times 10^3$ (cm/sec)	2.2	1.4	0.58	0.15
$D_p \times 10^6$ (cm^2/sec)	1.7	2.2	0.48	0.073
$D_q \times 10^6$ (cm^2/sec)	0.33	0.28	0.087	0.031

Data Reduction

The first and second moments were determined by fitting the response curve to the exponentially modified Gaussian function. The retention volume was calculated by subtracting the dead volume from the first moment. The peak variance was calculated by subtracting the variance of the system, measured without a column, from the second moment. Finally, the plate number N was calculated from the retention volume and the variance. The bed porosities ε for the Resource 15S (1 mL) and S HyperD 20 columns were determined form injections of a dextran conjugate (MW 8×10^6) dissolved in 1 M NaCl. The total porosity $\varepsilon_t = \varepsilon + (1 - \varepsilon)\varepsilon_p$ of a column was determined from the retention volume measured by injection of a very small volume of water using a 1 M $NaNO_3$ buffer. We have assumed that the porosities for the Q and S form of a resin are identical and that the two Resource 15S columns have identical porosities.

The retention volume at linear adsorbing condition is[14]

$$V_R = V_{col}\varepsilon[1 + k'] = V_{col}[\varepsilon + (1 - \varepsilon)K_d\varepsilon_p(1 + A)]$$
$$= V_{col}[\varepsilon + (1 - \varepsilon)K_d\varepsilon_p(1 + B_{C_s^{-\nu}})] \quad (6)$$

The three solute dependent retention parameters K_d, B, and ν were determined by fitting Eq. (6) to the experimental retention volumes at all counter ion concentration (Na^+ or Cl^-). For the cation exchange of aprotinin a concentration of 50 mM Na^+, originating from the acetate buffer, was added to the nominal salt concentration.

The mass transfer and axial dispersion coefficients were determined by fitting the van Deemter model, Eq. (1), with the parallel diffusion model, Eq. (4), to the experimental data for $h = L/Nd_p$ at all the counter ion concentrations and velocities using the smoothed expression for A obtained from Eq. (5). The film mass-transfer coefficient was correlated by the expression $k_f = \alpha v^\beta$, where α and β are constants. In the fitting procedure, global values of the exponent β and the axial dispersion parameter λ were applied.

RESULTS

Tyrosine

Figure 2 shows the variation of the experimental retention volumes with the salt concentration for tyrosine and aprotinin and the fit obtained with the model, Eq. (6). The retention volumes are scaled with the retention volume measured at nonretained conditions, i.e., at a high salt concentration. The porosities and retention parameters are reported in Table 1. The relative charge ν corresponds to the numerical value of the binding charge since the counter ions are monovalent. For tyrosine, the value of ν for both resins is close to the theoretical value of 1.9 at pH 11. This indicates that the entire charge of the amino acid molecule is involved in the adsorption. Figure 2 shows that the retention behavior for tyrosine on the two resins is almost identical.

The experimental plate height data and the fitted model at three velocities are shown in Figs. 3 and 4. The values for λ and the mass-transfer coefficients are shown in Table 1. The results obtained on the Resource 15Q resin exhibit the characteristic shape of parallel diffusion shown in Fig. l. The results obtained on the Q HyperD resin are somewhat scattered, which is often observed when the peak variance of a small solute molecule is determined on a column with a small volume, although the column–particle diameter ratio is

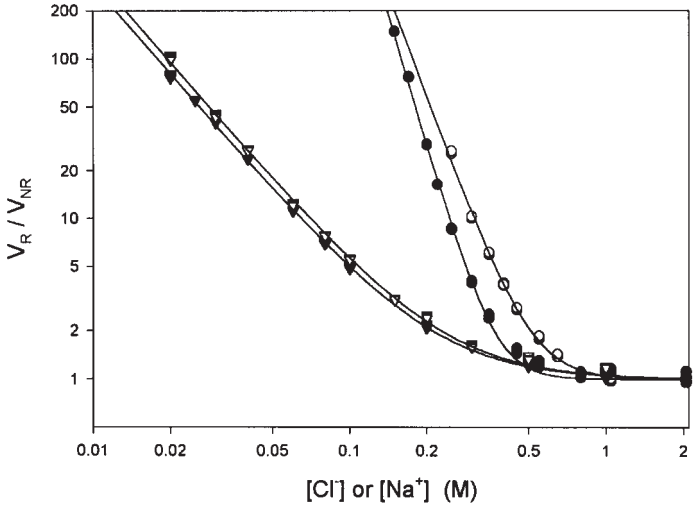

Figure 2. Experimental retention behavior of tyrosine (▽) and aprotinin (●) on Resource 15 (solid) and HyperD 20 (open) as a function of the counter ion concentration, [Cl^-] for tyrosine and [Na^+] for aprotinin. The lines are the retention volume model, Eq. (6).

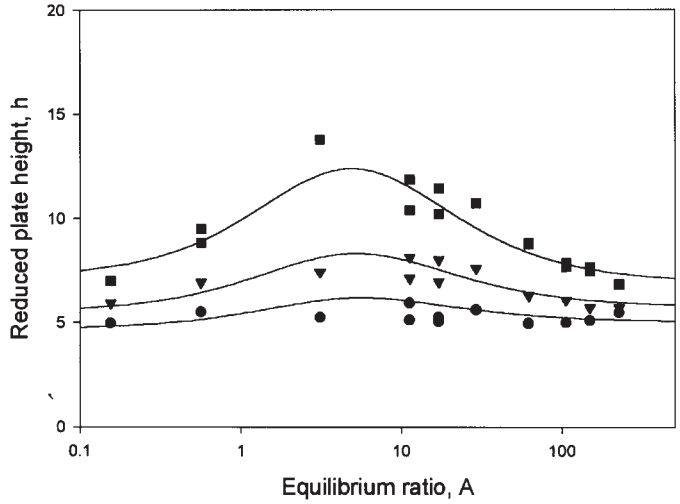

Figure 3. Experimental reduced plate heights for tyrosine on resource 15Q at superficial velocities of $v_0 = 0.05$ (●), 0.1 (▼), and 0.2 cm/sec (■). The lines are the parallel diffusion model.

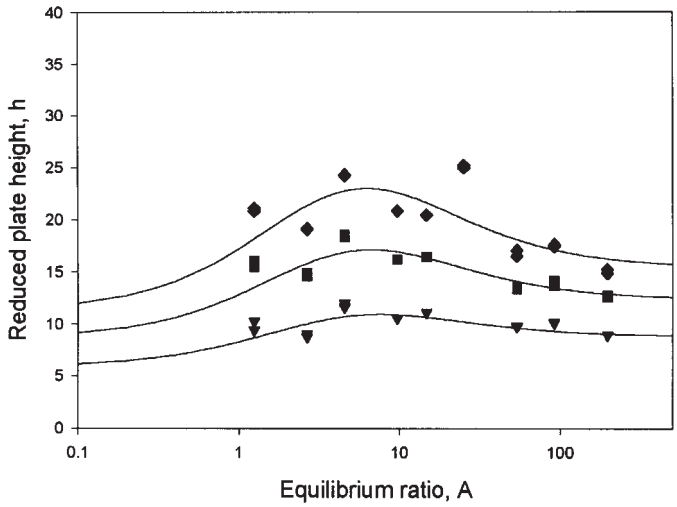

Figure 4. Experimental reduced plate heights for tyrosine on Q HyperD 20 at superficial velocities of $v_0 = 0.1$ (▽), 0.2 (●), and 0.3 cm/sec (◆). The lines are the parallel diffusion model.

above 200. The results show that neither the pore nor the solid diffusion model can describe the observed variation of the plate height with the equilibrium ratio. Only the parallel diffusion model fits the data satisfactorily.

Aprotinin

The relative binding charge for aprotinin is significantly larger than for tyrosine, therefore, the retention volumes for aprotinin increase more rapidly with decreasing salt concentration, as shown in Fig. 2. The difference in the retention on the two resins is more pronounced for aprotinin than for tyrosine owing to the difference in the charge ratio ν for aprotinin on the two resins, as reported in Table 1. Although it indicates that adsorption of aprotinin on the two resins does not involve the same number of charges, it is noted that the model parameters B and ν are strongly correlated and the true binding charges might therefore be more alike.

The variation of plate height with the equilibrium ration for aprotinin is shown in Figs. 5 and 6. Since aprotinin is a much larger molecule than tyrosine, a lower rate of mass transfer corresponding to a larger plate height is expected. Comparision of Figs. 5 and 6 with Figs. 3 and 4, shows that the plate height

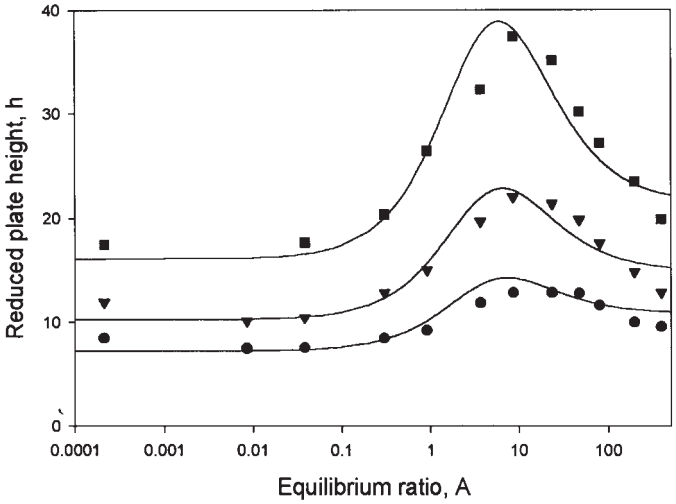

Figure 5. Experimental reduced plate heights for aprotinin on Resource 15S at superficial velocities of $v_0 = 0.05$ (●), 0.1 (▼), 0.2 cm/sec (■). The lines are the parallel diffusion model.

increased approximately by a factor of 3 on the Resource resin and a factor of 10 on the HyperD resin. For both resins, a maximum in the plate height is observed and a satisfactory fit is obtained using the parallel diffusion model. The 1 mL Resource column was used for $A > 40$ and the 6 mL column for $A < 40$, which may explain the discrepancies between the model and the data. Figure 7 shows a comparison of experimental and correlated reduced plate heights for aprotinin on Resource 15S at three different salt concentrations.

DISCUSSION

Evidently, when comparing the experimental results for tyrosine and aprotinin to the characteristic behavior of the three mass-transfer models, only the parallel diffusion model can describe the data satisfactory. The pore diffusion model predicts a monotonic increase of the plate height with retention approaching asymptotic values at strong and low retention; whereas, the solid diffusion model predicts a monotonic decrease of the plate height approaching an asymptotic value at strong retention.

In ion-exchange chromatography, the isotherms are linear at high salt concentrations but when the load is sufficiently high, they become nonlinear at moderate to low salt concentrations. The effect of nonlinearity of the

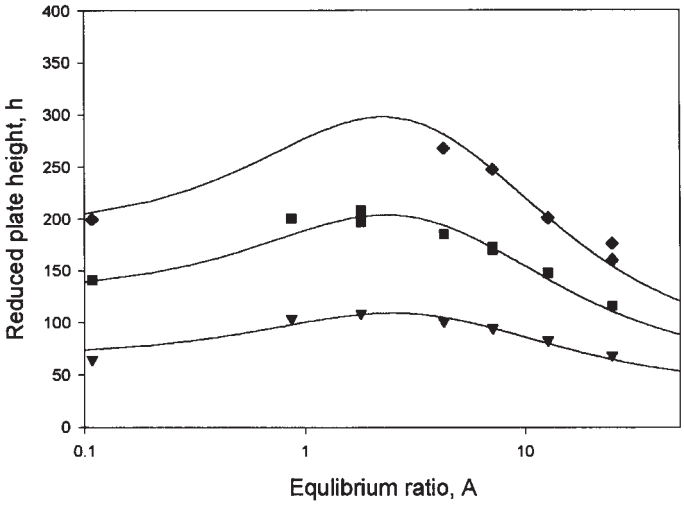

Figure 6. Experimental reduced plate heights for aprotinin on S HyperD 20 at superficial velocities of $v_0 = 0.1$ (▽), 0.2 (■), and 0.3 cm/sec (◆). The lines are the parallel diffusion model.

isotherm was, therefore, investigated. As expected, the experiments showed that a nonlinear isotherm has a much larger impact on the variance of the peak than on the retention volume. A significant increase in the load could reduce the retention volume by 5–10%, whereas, the variance could be increased by as much as 50%. Thus as the retention volume decreases and the variance increases and it will cause a significant increase in the plate height. This is in contrast to the decrease observed at moderate to strong retention shown in Figs. 3–6. Therefore, nonlinear effects cannot explain the observed plate height behavior. Figure 8 shows the shape of two aprotinin peaks at $v_0 = 0.1$ cm/sec on S HyperD 20 at $c_s = 0.25$ M corresponding to $A = 55$ and on Resource 15S at $c_s = 0.17$ M corresponding to $A = 196$. Even though the retention volumes are large, the peaks are almost symmetric.

Mass Transfer Behavior

The nature of solid diffusion is difficult to assess. In the solid diffusion model, the driving force is a concentration difference in the adsorbed state either at the inner surface of the porous particle (surface diffusion) or in the polymeric network of the gel-filled particle. It is not obvious whether solid

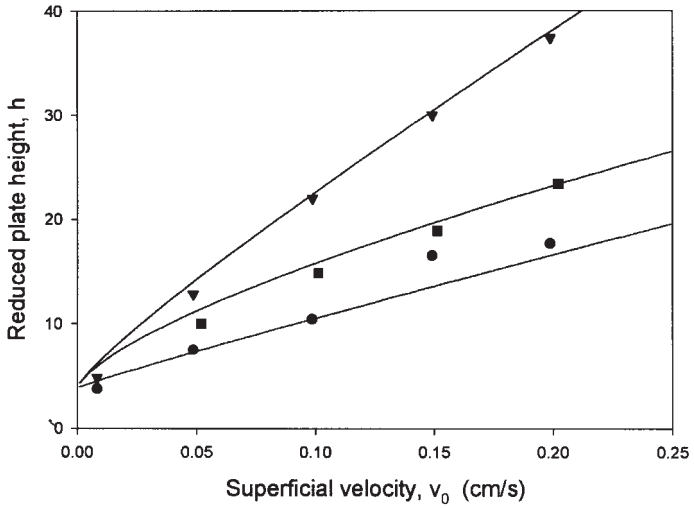

Figure 7. Experimental reduced plate heights for aprotinin on Resource 15S at salt concentrations of (●) 0.55, (▼) 0.30, and (■) 0.17 M NaCl. The lines are the parallel diffusion model.

diffusion is a physical phenomena or just a conceptual mechanism for describing a mass-transfer behavior deviating from pore diffusion. This issue should be considered in context with the fact that the models do not account for the principle of adsorption, in this case, ion exchange.

In the parallel diffusion model, the effective mass-transfer coefficient $k_p + Ak_q$ in the adsorbent depends on the equilibrium ratio and thus on the salt concentration. The diffusion coefficient of a charged solute depends on the salt concentration. Therefore, the parallel diffusion might instead originate from a concentration dependent diffusion coefficient. To investigate this possibility, we consider a model where the mass transfer occurs by pore diffusion and the diffusion coefficient in free solution is calculable from the Nernst–Planck equation

$$D_{\text{eff}} = \frac{D_A D_B (z_A^2 c_A + z_B^2 c_B)}{D_A z_A^2 c_A + D_B z_B^2 c_B} \tag{7}$$

A and B are the diffusing ion pairs, which in the present case, is either tyrosine and Na^+ or aprotinin and Cl^-. We assume that the relative change in the pore diffusion coefficient corresponds to the change in D_{eff}/D_A calculated from the Nernst–Planck equation. For aprotinin, the diffusion coefficient determined from the correlation by Young et al.[15] is $1.3 \times 10^{-6}\,\text{cm}^2/\text{sec}$ and Cl^-,

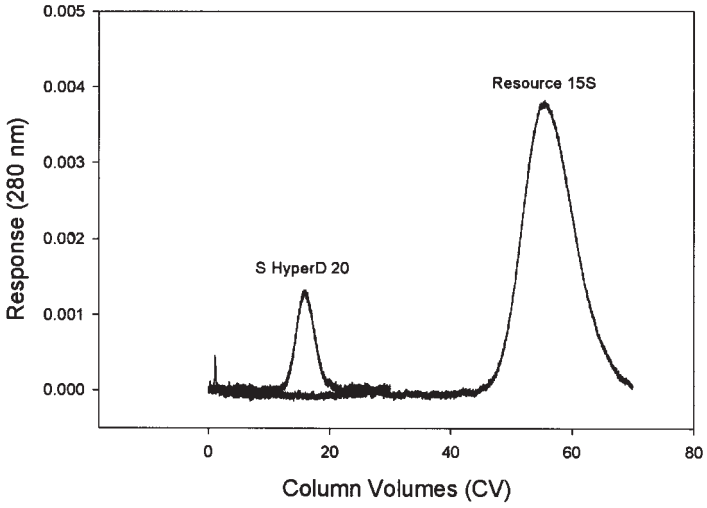

Figure 8. The shape of two aprotinin peaks at $v_0 = 0.1\,\mathrm{cm/sec}$ on S HyperD 20 at $c_s = 0.25\,\mathrm{M}$ corresponding to $A = 55$ and on Resource 15S at $c_s = 0.17\,\mathrm{M}$ corresponding to $A = 196$.

it is $20.3 \times 10^{-6}\,\mathrm{cm^2/sec}$.[13] The net charge z of aprotinin is 11. The largest value of the diffusion coefficient ratio is obtained when the solute concentration is high and the counter ion concentration low. Therefore, we inserted the feed concentration of aprotinin, $1\,\mathrm{g/L} = 0.15\,\mathrm{mM}$, and the lowest chloride concentration was applied, which is 100 mM. Inserting these numbers the diffusion coefficient ratio $D_{\mathrm{eff}}/D_{\mathrm{A}}$ for aprotinin becomes 1.54. For tyrosine, the diffusion coefficient, determined from the Wilke–Chang correlation, is $10 \times 10^{-6}\,\mathrm{cm^2/sec}$ and the value for Na^+ is $13.3 \times 10^{-6}\,\mathrm{cm^2/sec}$.[13] The lowest Na^+ concentration applied was 20 mM and the feed concentration of tyrosine was $0.3\,\mathrm{g/L} = 1.7\,\mathrm{mM}$. Inserting these concentrations and a charge of -1.9 for tyrosine, the calculated diffusion coefficient ratio $D_{\mathrm{eff}}/D_{\mathrm{A}}$ is 1.06. In comparison, the effective mass-transfer coefficient $k_{\mathrm{p}} + Ak_q$, which is proportional to the effective diffusion coefficient for the particle, varies by a factor of 20 for tyrosine on the Resource resin when the equilibrium ratio varies from 0 to 100. Thus, a concentration-dependent pore diffusion coefficient, as calculable from the Nernst–Planck equation, cannot account for the observed variation of the plate height.

Experimental studies of the plate height behavior of BSA on source 30Q in the range pH = 6–9 showed that the plate height depends on the equilibrium ratio but the mass-transfer coefficients k_{p} and k_q were shown to be independent of pH and the counter ion concentration.[14] A result that is

consistent with the model presented. The parallel diffusion model was used to describe the plate height behavior of organic solutes on reversed phase resins, where the adsorption mechanism is based on hydrophobicity and the mobile phase contains water, polar organic solvents, and modifiers.[11,16] Thus, the concept of parallel diffusion seems generally applicable and neither electrostatic effects (ion-exchange) nor hydrophobic effects (reversed phase) can explain the characteristic plate height behavior. It seems to depend on how strong the solute is attached to the ligands in the porous particles.

Parameter Evaluation

The estimated value for the axial dispersion parameter λ is between 1 and 2 corresponding to plate height contribution of 2–4 particle diameters. From the present experimental data, it was not possible to estimate robust parameters for α and β in the expression for the film coefficient $k_f = \alpha v^{\beta}$ because the film resistance is minor, except at strong retention, and because the variation of the velocity was not substantial enough to ensure a decoupling of α and β in the fitting procedure. Thus, the global value of $\beta = 1/3$ is somewhat arbitrary, although consistent with correlations[17,18] commonly used. The ratio of the α-parameters for tyrosine of aprotinin depends on the column characteristics only and should, therefore, be alike. The values in Table 1 show that this ratio is 4.2 for both solutes, which indicates that α has some physical significance and is not merely a fitting parameter.

To compare the two resins, the diffusion coefficients were calculated from the mass-transfer coefficients for the pore and solid phase using the relation $k_i = 10\,D_i/d_p$. The values are shown in Table 1. The solid diffusion coefficients are lower than the pore diffusion coefficients, which are significantly lower than the diffusion coefficients in free solution. The intraparticle diffusion coefficients for tyrosine in the Resource and the HyperD resins were similar, as indicated by the similar plate height behaviors, shown in Figs. 3 and 4. The diffusion coefficients for aprotinin in HyperD were smaller than the diffusion coefficients in Resource, especially the pore-diffusion coefficient. Although many factors influence the pore diffusivity, it is not unlikely that the diffusion of large molecules is more hindered in a gel-filled pore than in a nongel-filled pore. To ensure that the apparently low intraparticle diffusivities did not originate from the assumption that the Q and S media have the same porosities, experiments with tyrosine on S HyperD 20 at 1 M NaCl where performed. The retention and the plate height at 1 M NaCl on the S and the Q media were very similar, justifying the assumption of identical porosities. A significant difference in the apparent diffusion coefficients in the Resource and the HyperD resins was not only observed for

aprotinin. Similar studies with BSA showed that the maximum reduced plate height at a velocity of 0.1 cm/sec was approximately 150 in Resource 15Q and 500 in Q HyperD 20.[14]

Saunders et al.[19] used a batch up-take technique to investigate the pore and solid diffusion of tyrosine in an Amberlite 252 cation-exchange resin with a particle diameter of 800. Their estimated values are $D_p' = 2.3 \times 10^{-6}\,cm^2/sec$ sec and $D_q' = 0.018 \times 10^{-6}\,cm^2/sec$, where $D_i' = K_d \varepsilon_p D_i$. Using the same experimental approach, Jones and Carta[20] determined solid-diffusion coefficients for various amino acids on seven different Dowex resins with particle diameters in the range of 450–850 μm. Their values of D_q' for phenyl alanine, which resembles tyrosine, are in the range of $0.02–0.1 \times 10^{-6}\,cm^2/sec$, with one exception of $3 \times 10^{-6}\,cm^2/sec$. Our values for tyrosine are $D_p' = 0.84$ and $1.2 \times 10^{-6}\,cm^2/sec$ and $D_q' = 0.17$ and $0.15 \times 10^{-6}\,cm^2/sec$ in Resource and HyperD, respectively.

The primary application of the van Deemter equation is to characterize and, thereby, compare different resins, and often, approximate shortcut methods with a minimum number of experiments are needed. In regard to this, an interesting observation can be made from the present study: If an approximate expression for the plate height as a function of the velocity and the retention factor is needed, it is better to use the van Deemter equation in the simple form $H = A + Cv$, where A and C are constants, than to use Eq. (1), with a constant overall mass-transfer coefficient K_m. The reason is that the term $[k'/(1 + k')]^2$ varies to a much greater extent than the experimental plate height because K_m varies with the retention. If K_m was a constant, the variation of the plate height with retention would correspond to the pore diffusion model in Fig. 1, and this is not what we observed experimentally. The experimental data in Figs. 3–6 indicate that an appropriate average number for C can be determined from a flow rate study at a retention in the range of $k'1–2$. For many proteins, this corresponds to a NaCl concentration in the range of 0.3–0.4 M

CONCLUSION

The mass-transfer behavior of the polypeptide aprotinin and the amino acid tyrosine was investigated on the porous resin Resource 15 and the gel-filled resin HyperD 20 by determining the plate height as a function of the equilibrium ratio and velocity. The observed variation of the plate height with retention cannot be described by a model containing either pore or solid diffusion as the rate mechanism. But when combining the two mechanisms into a parallel diffusion model, a satisfactory agreement between the model and the experimental data was obtained. Although

it is not obvious whether parallel diffusion is a physical phenomena or just a conceptual mechanism for describing mass-transfer behavior in chromatographic media, we find the use of two intraparticle mass-transfer coefficients for modelling the intraparticle mass-transfer substantiated by the experimental work.

SYMBOLS

A	Equilibrium ratio
B	Lumped equilibrium parameter (M^v)
c	Solute concentration in the mobile phase (M)
c_{pore}	Solute concentration in the pores (M)
c_s	Salt ion concentration (M)
D	Diffusion coefficient in free solution (cm^2/sec)
D_p	Pore diffusion coefficient (cm^2/sec)
D_q	Solid diffusion coefficient (cm^2/sec)
K	Equilibrium constant
K'	Retention factor
K_d	Steric exclusion factor
k_f	External mass-transfer coefficient (cm/sec)
K_m	Overall mass-transfer coefficient (cm/sec)
k_p	Pore mass-transfer coefficient (cm/sec)
k_q	Solid mass-transfer coefficient (cm/sec)
p	Constant, $\varepsilon/(1-\varepsilon)K_d\varepsilon_p$
q	Adsorbed phase concentration (M)
v	Interstitial velocity (cm/sec)
v_0	Superficial velocity (cm/sec)
V_R	Retention volume mL
V_{NR}	Retention volume at non-retained conditions, i.e., $A = 0$ (mL)

Greek Letters

α	External mass transfer parameter
β	Velocity exponent
ε	Bed porosity
ε_p	Particle porosity
Λ	Capacity
λ	Axial dispersion parameter
ν	Charge ratio

ACKNOWLEDGMENT

Aprotinin was kindly provided by Ole Schou, *Protein Purification*, Novo Nordisk A/S, Denmark.

REFERENCES

1. Nash, D.C.; Chase, H.A. Comparison of diffusion and diffusion-convection matrices for use in ion-exchange separations of proteins. J. Chromatogr. A **1998**, *807*, 185–207.
2. Rodrigues, A.E.; Chenou, C.; de la Vega, M.R. Protein separation by liquid chromatorgraphy using permeable POPOS Q/M particles. Chem. Eng. J. **1996**, *61*, 191–201.
3. Horvarth, J.; Boschetti, E.; Guerrier, L.; Cooke, N. High-performance protein separations with novel strong ion exchangers. J. Chromatogr. A **1994**, *679*, 11–22.
4. van Deemter, J.J.; Zuiderweg, F.J.; Klinkenberg, A. Longitudinal diffusion and resistance to mass transfer as causes of nonideality in chromatography. Chem. Eng. Sci. **1956**, *5*, 271–289.
5. Yamamoto, S.; Nakanishi, K.; Matsuno, R. *Ion-Exchange Chromatography of Proteins*; Marcel Dekker: 1988; 315.
6. Perry, R.H.; Green, D.W. Adsorption and ion exchange. In *Perry's Chemical Engineers' Handbook*, 7th Ed.; McGraw-Hill: New York, 1997; Chap. 16.
7. Chu, C.F.; Ng, K.M. Flow in Packed tubes with a small tube to particle diameter ratio. AIChE J. **1989**, *35*, 148–158.
8. Chung, S.F.; Wen, C.Y. Longitudinal dispersion of liquid flowing through fixed and fluidized beds. AIChE J. **1968**, *14*, 857–866.
9. Gunn, D.J. Axial and radial dispersion in fixed beds. Chem. Eng. Sci. **1987**, *42*, 363–373.
10. Knox, J.H. Band dispersion in chromatography—a new view of A-term dispersion. J. Chromatogr. A **1999**, *831*, 3–15.
11. Knox, J.H.; Scott, H.P. B and C terms in the van Deemter equation for liquid chromatography. J. Chromatogr. **1983**, *282*, 297–313.
12. Brooks, C.A.; Cramer, S.M. Steric mass-action ion-exchange—displacement profiles and induced salt gradients. AIChE J. **1992**, *38*, 1969–1978.
13. Atkins, P.W. *Physical Chemistry*, 4th Ed.; Oxford University Press, 1990.
14. Hansen, E. Application of the Linear Driving Force Approximation to the Study of Mass Transfer in Ion Exchange Chromatography; Department of Chemical Engineering, Technical University of Denmark, 2000; Ph. D. Thesis.

15. Young, M.E.; Carroad, P.A.; Bell, R.L. Estimation of diffusion coefficients of proteins. Biotechnol. Bioeng. **1980**, *22*, 947–955.
16. Stout, R.W.; DeStefano, J.J.; Snyder, L.R. High-performance liquid chromatographic column efficiency as function of particle composition and geometry and capacity factor. J. Chromatogr. **1983**, *282*, 263–286.
17. Kataoka, T.; Yoshida, H.; Ueyama, K. Mass transfer in laminar region between liquid and packing material surface in packed bed. J. Chem. Eng. Japan **1972**, *38*, 132–136.
18. Wilson, E.J.; Geankoplis, C.J. Liquid mass transfer at very low reynolds numbers in packed beds. Ind. Eng. Chem. Fundamen. **1966**, *5*, 9–14.
19. Saunders, M.S.; Vierow, J.B.; Carta, G. Uptake of phenylalanine and tyrosine by a strong-acid cation exchanger. AIChE J. **1989**, *35*, 53–68.
20. Jones, I.L.; Carta, G. Ion-exchange of amino-acids and dipeptides on cation resins with varying degree of cross-linking. 2. Intraparticle transport. Ind. Eng. Chem. Res. **1993**, *32*, 117–125.